

# Enhancement of proton mobility and mitigation of methanol crossover in sPEEK fuel cells by an organically modified titania nanofiller

Catia de Bonis<sup>1</sup> · Cataldo Simari<sup>2</sup> · Vasiliki Kosma<sup>2</sup> · Barbara Mecheri<sup>1</sup> ·  
Alessandra D'Epifanio<sup>1</sup> · Valentina Allodi<sup>3</sup> · Gino Mariotto<sup>3</sup> · Sergio Brutti<sup>4</sup> ·  
Sophia Suarez<sup>5</sup> · Kartik Pilar<sup>6</sup> · Steve Greenbaum<sup>6</sup> · Silvia Licoccia<sup>1</sup> · Isabella Nicotera<sup>2</sup>

Received: 3 June 2015 / Revised: 26 October 2015 / Accepted: 22 February 2016 / Published online: 29 February 2016  
© Springer-Verlag Berlin Heidelberg 2016

**Abstract** An organically functionalized titania,  $\text{TiO}_2\text{-RSO}_3\text{H}$ , was evaluated as filler in sulfonated polyetheretherketone (sPEEK)-based composite membranes for application in high temperature direct methanol fuel cells. The presence of propylsulfonic acid groups covalently bound onto the  $\text{TiO}_2$  surface and the nanometric nature of the additive were analyzed by Raman spectroscopy and transmission electron microscopy, respectively. The properties of the sPEEK/ $\text{TiO}_2\text{-RSO}_3\text{H}$  composite membranes were compared with those of the pure sPEEK membranes and those of the sPEEK/ $\text{TiO}_2$  composite membranes containing pristine titania nanoparticles at same filler content. Water and methanol transport properties were investigated by NMR methods, including relaxation times and self-diffusion coefficients as function of temperature (up to 130 °C), and pressure (from 0 up to 2 kbar). The incorporation of the nanoadditives in the sPEEK polymer demonstrates considerable effects on the morphology and stiffness of

the membranes, as well as on the transport properties and barrier effect to the methanol crossover. In particular, the functionalization by propylsulfonic acid groups promotes a higher reticulation between the polymeric chains, increasing the tortuosity of the methanol diffusional paths, so reducing the molecular diffusion, while the proton mobility increases being favored by the Grotthus-type mechanism. Conductivity measurements point out that the filler surface functionalization avoids the reduction of the overall proton conduction of the electrolyte due to the embedding of the low-conducting  $\text{TiO}_2$ . Finally, remarkable improvements were found when using the sPEEK/ $\text{TiO}_2\text{-RSO}_3\text{H}$  composite membrane as electrolyte in a DMFC, in terms of reduced methanol crossover and higher current and power density delivered.

**Keywords** sPEEK · Nanocomposites · Organically functionalized titania nanoparticles · NMR · DMFC

✉ Isabella Nicotera  
isabella.nicotera@unical.it

<sup>1</sup> Department of Chemical Science and Technologies, University of Rome “Tor Vergata”, Via della Ricerca Scientifica, 00133 Rome, Italy

<sup>2</sup> Department of Chemistry and Chemical Technologies, University of Calabria, Via P. Bucci, 87036 Rende (CS), Italy

<sup>3</sup> Dipartimento di Informatica, Università di Verona, Strada Le Grazie 15, 37134 Verona, Italy

<sup>4</sup> Dipartimento di Scienze, Università della Basilicata, V.le dell'Ateneo Lucano 10, 85100 Potenza, Italy

<sup>5</sup> Department of Physics, Brooklyn College/CUNY, Brooklyn, NY 11210, USA

<sup>6</sup> Department of Physics and Astronomy, Hunter College of the City University of New York, New York, NY 10065, USA

## Introduction

Direct methanol fuel cells (DMFC) have been recently considered as promising power sources for portable and transport applications due to their high efficiency, high power density, compact cell design, and low emissions [1, 2]. Proton exchange membranes (PEMs) are the key components of a DMFC: PEMs transfer protons from the anode to the cathode and act as a barrier to fuel crossover. However, technological barriers still need to be overcome for DMFC large-scale commercialization. In particular, methanol permeation through the membrane [3] is one of the most serious limitations since it leads to reduced energy conversion efficiency due to the direct chemical oxidation of methanol in the cathodic half-cell, and also causes cell operational failures.

Nafion is the most widely used membrane material due to its high thermal stability and good mechanical and electrochemical properties. However, it suffers a high permeability to methanol as well as a major decrease of the proton conductivity above 80 °C at low humidity, thus limiting its use in DMFCs. Several strategies have been developed to improve the performance of Nafion membranes, including the preparation of composites containing organically modified inorganic fillers, such as silica, clays, and graphene oxide [4–7].

The use of an organic-inorganic hybrid compound offers the possibility to combine in a single material both the thermal and mechanical stability of inorganic component and the characteristic chemical of organic functional groups. The grafting of proper organic moieties on the filler surface reduces the proton conductivity loss of Nafion induced by the embedding of low-conducting inorganic particles. Furthermore, the enhanced interfacial compatibility with polymeric matrix can favor the uniform dispersion of filler at a nanometric scale level.

Recently, we have investigated composite membranes containing organically modified titanium oxides, thus obtaining electrolytes with better mechanical properties, reduced methanol permeability, and higher power density delivered in a DMFC, with respect to unfilled Nafion membranes [8, 9].

In the present work, this filler was tested in a polymer different from Nafion and a more comprehensive NMR analysis was performed, including the use of hydrostatic pressure as a thermodynamic variable, in order to understand the effect of the filler on the transport properties of methanol and water, and its interaction with this polymer. In fact, the use of hydrocarbon polymers alternative to Nafion is still one of the main targets to develop cheaper proton exchange membranes and with lower methanol permeability [10]. Aromatic main chain polymers such as poly(ether ketone), poly(phenylene sulphone), poly(ether sulphone), and poly(benzimidazoles) have been extensively studied as they are low-cost and high-performance materials that can be chemically modified to obtain proton-conducting electrolytes [11–14]. Among them, sulfonated polyetheretherketone (sPEEK) is interesting for applications in DMFCs because its microstructure consists of narrower and less connected water-filled channels compared to those of Nafion, and this can help to reduce the problems related to methanol crossover and high water drag that occur in cell operative conditions [15]. The degree of sulfonation (DS) of sPEEK is a crucial parameter for its performance because the proton conductivity increases with the increment of DS, but the methanol crossover also increases, and the dimensional stability of the membrane worsens up to dissolution because of the excessive hydrophilicity of the ionomer.

Different methods have been developed to improve the proton conductivity limiting dimensional changes of sPEEK membranes, including the introduction of specific functional

groups onto the ionomer backbone, and the preparation of polymer blends and organic-inorganic composites [15–18]. However, a limited attention has been focused on the investigation of the microstructural modifications of the ionomer in relation to the use of these strategies. The pristine sPEEK membrane has a distinct structuring and nanomorphology arising from self-organization of the sulfonated polymer chains into hydrophilic and hydrophobic domains. Concerning organic-inorganic composites, the embedding of inorganic component will affect the structure of water-filled channel network, and hence the permeability to methanol and proton transport properties of the electrolyte [19, 20].

In this work, sPEEK having DS = 0.5 has been used as polymeric matrix to obtain composite membranes with adequate proton conductivity and good mechanical properties. Propylsulfonic-functionalized nanometric titania ( $\text{TiO}_2\text{-RSO}_3\text{H}$ ) has been used as filler, in which aliphatic chains ending with sulfonic acid groups are covalently bound onto the oxide surface. The nanometric nature of the filler and the presence of bifunctional branches can increase the chemical-physical interactions with the polymer matrix. This is expected to favor the proton transport through the Grotthus-type mechanism, and to limit the vehicular transport mechanism, that facilitates methanol permeation through the membrane.

Fillers and membranes morphologies have been studied by transmission electron microscopy (TEM) and atomic force microscopy (AFM), respectively, and the vibrational features of the silylpropylsulfonic-functionalization on the grafted titania surfaces by Raman spectroscopy (RS).

The transport properties of water and methanol confined within the sPEEK and composite membranes have been studied by NMR methods in order to understand the molecular dynamics through direct measurement of the self-diffusion coefficients ( $D$ ) and relaxation times ( $T_1$ ) in a wide temperature range (25–130 °C). The goal is to evaluate how the ionic conduction is influenced by the polymeric structure and the nanofillers. Self-diffusion measurements on water and methanol have been also carried out under variable hydrostatic pressure conditions in order to probe molecular motion and ionic diffusion processes associated with temperature-independent volume fluctuations [21–24].

Finally, electrochemical characterization was carried out on the membranes to investigate their performance in fuel cell operative conditions. The influence of surface functionalization of the filler on proton conductivity of the membranes was probed by using ac impedance spectroscopy. The functioning of these membranes in a real device, in terms of current and power density delivered, was tested by polarization measurements and their methanol permeability was evaluated by using linear sweep voltammetry.

## Experimental section

### Materials

Polyetheretherketone (PEEK, 450 PF, MW = 38,300 g/mol, 132 repeat units per mole) was purchased in powder form from Victrex. Pt (20 wt.%) and Pt/Ru (60 wt.%) black powders were supplied from Alfa Aesar. Nafion perfluorinated resin solution (5 wt.% in a mixture of lower aliphatic alcohols and water), polytetrafluoroethylene (PTFE), tetrabutylammonium hydroxide (TBAOH), and all other chemicals were purchased from Sigma-Aldrich.

### Synthesis of fillers and sPEEK

Titania powder was prepared as previously described [25] to obtain the nanostructured oxide in the anatase phase with surface hydroxyl groups, such as to allow its subsequent functionalization. The surface chemistry of the oxide was investigated by X-ray photoelectron spectroscopy (XPS) and the relative peak area associated with of the oxygen species of the surface OH groups resulted to be 21 versus 73 % of the peak deriving from O-Ti-O species of the framework.

The preparation of  $\text{TiO}_2\text{-RSO}_3\text{H}$  was then carried out following a two-step synthetic pathway: (i) introduction of mercaptopropyl moieties onto titania surface; (ii) subsequent oxidation of the thiol groups into sulfonic acid groups to obtain propylsulfonic-functionalized titania [8]. The amount of functional groups in  $\text{TiO}_2\text{-RSO}_3\text{H}$  was determined by CHNS/O elemental analysis and neutron activation analysis (NAA) and was 2 wt.%, corresponding to 0.12 mmol/g.

sPEEK was prepared via aromatic electrophilic substitution following the procedure previously reported [16]. PEEK was reacted with  $\text{H}_2\text{SO}_4$  (96 %) controlling the temperature and reaction time. The degree of sulfonation of the product was evaluated by  $^1\text{H}$  NMR and by titration and resulted to be  $\text{DS} = 0.5$ .

### Preparation of electrodes

The gas diffusion layer (GDL) was prepared according to the following procedure. A solution of water (4 mL), isopropyl alcohol (5.1 mL), and Vulcan XC-72R carbon black (0.25 g) was kept under magnetic stirring for 10 min and then mixed under sonication for 10 min. Twenty-nine microliters of PTFE (60 wt.% in water) was added to the mixture that was kept under magnetic stirring for 10 min and mixed under sonication for 15 min. The solution was airbrushed on a carbon paper containing 30 wt.% of PTFE, until reaching a load of carbon black of  $4.5 \text{ mg/cm}^2$ . The electrode was pressed for 30 min at  $90^\circ\text{C}$  under a load of  $20 \text{ kg/cm}^2$  and put in oven at  $70^\circ\text{C}$  for 30 min, at  $120^\circ\text{C}$  for 30 min, at  $280^\circ\text{C}$  for 15 min, and at  $350^\circ\text{C}$  for 30 min.

The ink of anode catalyst was prepared as follows. A slurry made of 6.7 mg of Pt/Ru powder and  $61.1 \mu\text{L}$  of Nafion solution was kept under stirring for 1 h. Then, 26.7 mg of glycerol and 3.22 mg of TBAOH were added and the mixture was stirred for 1 h. Finally, 22 mg of glycerol was added and the solution was kept under stirring overnight.

The ink of cathode catalyst was prepared as follows. A slurry composed of 5 mg of Pt powder and  $45.8 \mu\text{L}$  of Nafion solution was stirred for 1 h. Then, 20 mg of glycerol and 2 mg of TBAOH were added and the mixture was stirred for 1 h. Finally, 16 mg of glycerol was added and the solution was kept under stirring overnight.

The inks were distributed on the electrodes with GDL and dried overnight. The anode was prepared with a Pt/Ru loading of  $4 \text{ mg/cm}^2$  and the cathode with a Pt loading of  $1 \text{ mg/cm}^2$ . The electrodes were pressed for 5 min at  $90^\circ\text{C}$  under a load of 1 t and treated in a standard activation procedure using  $\text{H}_2\text{O}_2$  3 vol.% solution, 0.5 M  $\text{H}_2\text{SO}_4$  solution and distilled water, boiling the samples for 1 h in each solution.

### Preparation of membranes

sPEEK-based composite membranes containing 10 wt.% of  $\text{TiO}_2$  or  $\text{TiO}_2\text{-RSO}_3\text{H}$  were prepared by solution casting. In a typical procedure, sPEEK (250 mg) was dissolved in DMAc (20 mL) and the resulting solution was added to the filler/DMAc solution. The mixture was then heated to  $80^\circ\text{C}$  under stirring until the volume was reduced to 5 mL, cast onto a Petri plate, and heated to  $80^\circ\text{C}$  overnight. Pure sPEEK membranes were also prepared. The membranes selected for polarization and methanol permeability tests had a thickness of ca.  $100 \mu\text{m}$ . Before any characterization, all the membranes were treated in a standard activation procedure using 0.5 M  $\text{H}_2\text{SO}_4$  solution and distilled water [16].

### Characterization techniques

**Microscopy and Raman spectroscopy** TEM experiment was carried out on a FEI G2 20 HR-TEM equipped with a  $\text{LaB}_6$  electron beam source, two 2D flat cameras (low resolution and high resolution) and a cold finger for cryo-TEM experiments. Sample powders were suspended in hexane by repeated treatment in an ultrasonic bath and adsorbed on copper holey carbon film grids. TEM experiments were carried out at 200-kV electron energy and in cryo-conditions.

Atomic force microscopy (AFM) experiments were carried out by a Park AFM XE120 instrument equipped with a home-modified universal closed liquid cell to allow careful control of the RH condition upon scanning. Measurements were performed at  $\text{RH} = 33\%$ . Prior to the AFM tests, membranes were fully conditioned for 30 days in a closed vessel at 33 % relative humidity (RH, water vapor back pressure above a

saturated aqueous  $\text{MgCl}_2$  solution). The AFM study was carried out in tapping intermittent contact mode (TM). It is important to underline that phase-distance curves were carefully monitored upon imaging in order to avoid unstable regimes [26] and the rise of height artifacts in AFM topographies. Topographies and phase images were simultaneously recorded. Only phase images are reported in this communication because the membrane elastic response is highly sensitive to transitions from hydrophobic to hydrophilic domains, and thus, phase image is much more informative than topography. AFM images were recorded of both sides of the two membranes to highlight possible differences: three different areas were sampled on all membrane sides by recording at least five different magnifications in each zone. AFM images were analyzed using ImageJ software [27, 28] in order to study the evolution of the size of the hydrophobic and hydrophilic domains. Our procedure required the analysis of at least three phase images with different magnification and the identification of more than 300 pseudo-particles (hydrophobic and hydrophilic) for each. The size of the recorded particles were then analyzed by deriving for each membrane the particle size distribution and the cluster dimension mean values for both hydrophobic and hydrophilic domains.

Micro-Raman spectroscopy measurements were carried out in backscattering geometry using a single-stage Horiba-Jobin Yvon spectrometer (model LABRAM HR), coupled to a He-Ne laser as excitation source (at 632.8 nm) and a notch filter for the Rayleigh line cutoff. The scattered radiation was dispersed by a diffraction grating having 600 lines/mm and detected at the spectrograph output by a multichannel detector, a CCD with  $1024 \times 256$  pixels, cooled by liquid nitrogen, and with its maximum efficiency occurring in the red region. The wavenumber limit, due to the notch filter, was about  $200 \text{ cm}^{-1}$  on the low-energy side.

**NMR spectroscopy** NMR measurements were performed on a Bruker NMR spectrometer AVANCE 300 Wide Bore working at 300 MHz on  $^1\text{H}$ . The employed probe was a Diff30 Z-diffusion 30 G/cm/A multinuclear with substitutable RF inserts. Spectra were obtained by transforming the resulting free-induction decay (FID) of single  $\pi/2$  pulse sequences. The pulsed field gradient stimulated-echo (PFG-STE) method [29] was used to measure self-diffusion coefficients. This sequence is generally applied when the materials are characterized by a transverse relaxation time ( $T_2$ ) considerably shorter than longitudinal relaxation time ( $T_1$ ). The sequence consists of three  $90^\circ$  rf pulses ( $\pi/2-\tau_1-\pi/2-\tau_m-\pi/2$ ) and two gradient pulses that are applied after the first and the third rf pulses, respectively. The echo is found at time  $\tau = 2\tau_1 + \tau_m$ . Following the usual notation, the magnetic field gradient pulses have

magnitude  $g$ , duration  $\delta$ , and interpulse time delay  $\Delta$ . The attenuation of the echo amplitude is represented by the following (Eq. 1):

$$I(2\tau_1 + \tau_m) = \frac{1}{2} I_0 \exp \left[ -\frac{\tau_m}{T_1} - \frac{2\tau_1}{T_2} - (\gamma g \delta)^2 D \left( \Delta - \frac{\delta}{3} \right) \right] \quad (1)$$

where  $D$  is the self-diffusion coefficient. The used experimental parameters were gradient pulse length  $\delta = 1 \text{ ms}$ , time delay  $\Delta = 10 \text{ ms}$ , and the gradient amplitude varied from 100 to  $800 \text{ G cm}^{-1}$ . The uncertainty in the self-diffusion measurements is  $\sim 3 \%$ .

Longitudinal relaxation times ( $T_1$ ) of water and methanol were measured by the inversion-recovery sequence ( $\pi-\tau-\pi/2$ ). Both self-diffusion and  $T_1$  measurements were conducted by increasing temperature step by step from 20 to  $130 \text{ }^\circ\text{C}$ , with steps of  $20 \text{ }^\circ\text{C}$ , and allowing the sample to equilibrate for about 15 min. All the membranes, before the NMR measurements, were dried in oven, weighed and then immersed in water and in aqueous methanol solutions (2 M concentration) at room temperature. Upon being removed from the water, they were quickly blotted dry with a paper tissue (to eliminate most of the free surface liquid). The solvent content value was determined using a microbalance and recorded as described in the following formula (Eq. 2):

$$wu\% = \left[ (m_{\text{wet}} - m_{\text{dry}}) / m_{\text{dry}} \right] \times 100 \quad (2)$$

At this point the membranes were loaded into a 5 mm NMR Pyrex tube.

High-pressure diffusion measurements were done on a Varian NMR spectrometer and an Oxford 300 Wide Bore magnet. A custom built Cu-Be probe was used with a Harwood Engineering high pressure pump to reach pressures of up to 2000 bar. 3M's Fluorinert FC-3283 electronic fluid was used as the hydraulic fluid to avoid hydrogen background. In order to isolate the membrane from the pressure-transmitting fluid, the samples were sealed in a polyethylene sheath. Due to the nature of the Cu-Be pressure vessel, the pulsed field gradient method cannot be used to obtain diffusion measurements [23]. Instead, the probe was lowered from the homogeneous field of the magnet into the fringe field, where the field strength was 1.9 T and the static magnetic field gradient was measured using the known self-diffusion coefficient of liquid water to be  $g = 30.041 \text{ T m}^{-1}$ . Diffusion measurements were made using a Hahn spin-echo pulse sequence ( $\pi/2-\tau-\pi-\tau$ ) [30]. Echo intensity was measured as a function of  $\tau$ . The attenuation in echo intensity using the static field gradient was as follows (Eq. 3):

$$I(2\tau) = I_0 \exp \left[ \frac{-2\tau}{T_2} \right] \exp \left[ \frac{-2}{3} \gamma^2 \tau^3 g^2 D \right] \quad (3)$$

Heating tape around the probe and a thermocouple connected to a temperature controller allowed for temperature to be controlled simultaneously with high pressure.

**Mechanical tests** Dynamic mechanical analysis (DMA) measurements were made with a Metravib DMA/25 equipped with a shear jaw for films. Spectra were collected by applying a dynamic strain of amplitude  $10^{-3}$  at 1 Hz in the temperature range between 25 and 250 °C with a heating and cooling rate of 2 °C/min.

**Ion exchange capacity measurements** The ion exchange capacity (IEC) was determined by an acid-base titration. Disks of the membranes with known dry mass were equilibrated in 1.0 M NaCl aqueous solution for 24 h to replace the  $H^+$  by  $Na^+$  ions. The solution was titrated with 0.1 M NaOH (Aldrich, volumetric standard) using phenolphthalein as an indicator. IEC values ( $meq\ g^{-1}$ ) were calculated by the following (Eq. 4):

$$IEC = \frac{V_{NaOH} \times C_{NaOH}}{m_{dry}} \quad (4)$$

where  $V_{NaOH}$  is the added titrant volume at the equivalent point (mL),  $C_{NaOH}$  is the molar concentration of the titrant, and  $m_{dry}$  is the dry mass of the sample (g).

**Conductivity** Through-plane proton conductivity was measured by electrochemical impedance spectroscopy (EIS) using a multichannel potentiostat (VMP3 BioLogic Science Instruments). Disks of membranes were sandwiched between gas diffusion electrodes (E-Tek ELAT HT 140E-W with a Pt loading of  $5\ mg\ cm^{-2}$ ). The proton conductivity was measured as a function of temperature at saturated water vapor pressure (100 % relative humidity (RH)) in the frequency range from 1 Hz to 1 MHz, at an applied voltage of 25 mV. Before measurements, the samples were equilibrated overnight at room temperature and RH = 100 %.

**DMFC tests and MeOH permeation measurements** Membrane electrode assemblies (MEAs) were formed by hot-pressing the electrodes onto the membrane for 5 min at 120 °C under a load of 1 t and placed in a single cell (Fuel Cell Technologies, Inc.) with active area of  $5\ cm^2$ . A home-made test station was used to evaluate the MEA performance, feeding the cathode with humidified oxygen and the anode with a 2 M methanol solution. The feed supply of methanol was monitored by a KNF's Model FEM 1.10 TT.18 S diaphragm metering pump (flow rate  $2\ mL\ min^{-1}$ ). The oxygen supply was controlled by a MKS PR4000 mass-flow controller (flow rate 150 sccm), and the humidifier temperature was set to ensure 100 % RH of the gas. A pressure of 1 abs bar at both anode and cathode was used at 70 °C, whereas it was

increased up to 2 abs bar at 90 °C. Polarization and power density curves were obtained using a Multichannel Potentiostat (VMP3 BioLogic Science Instruments).

Methanol permeation was evaluated by linear sweep voltammetry, measuring the steady-state limiting current density at cathode due to the oxidation of methanol permeating from the anode side. The anode was fed by 2 M methanol solution, and humidified  $N_2$  was fed to the cathode. Limiting current density ( $J_{lim}$ ) was measured applying a voltage from 0 to 1.3 V (scan rate  $2\ mV\ s^{-1}$ ).

## Results and discussion

### Morphological and spectroscopic investigation

The strong acid  $-SO_3H$  groups were covalently bound onto the  $TiO_2$  surface by bifunctional branches to enhance the proton conductivity of the oxide and to favor the interfacial interactions with polymer matrix to obtain a more uniform dispersion of filler in composite membranes.

$TiO_2$  and  $TiO_2-RSO_3H$  were preliminarily characterized by studying their physicochemical properties by completing the picture already published by some of us in [8].

Transmission electron micrographies of the bare and grafted nanoparticles are shown in Fig. 1.

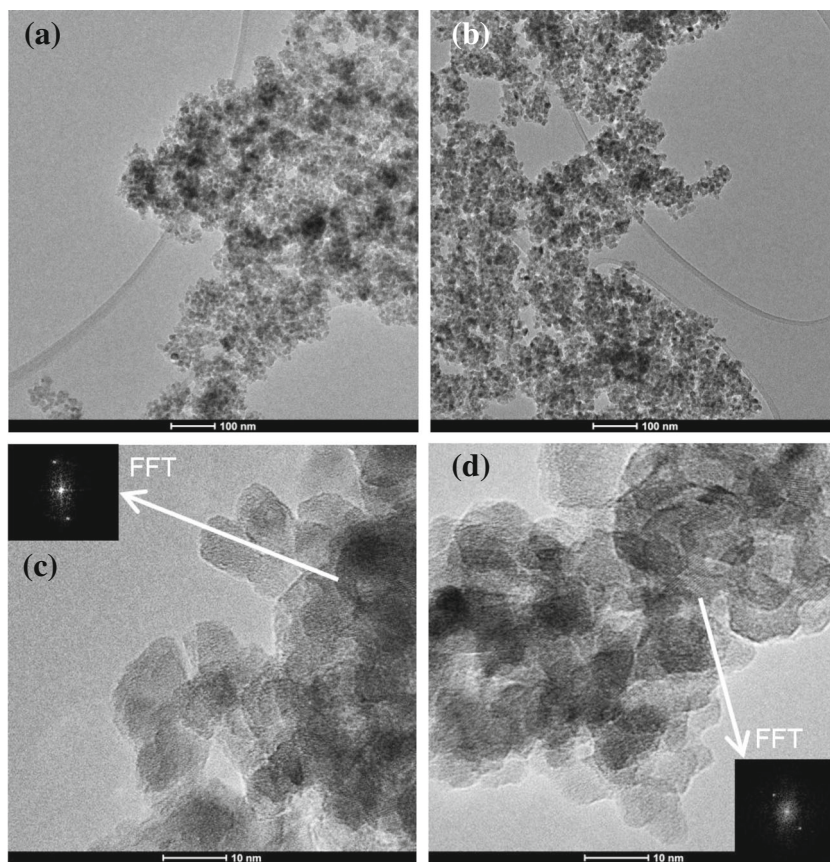
Samples are consist of nanometric round-shaped particles with very similar pseudospheric diameter. The two powders were morphologically very pure: no contaminations by larger particles, chunks, or other morphologies have been highlighted. The nanoparticle sizes are very homogenous: mean diameters of about 8–9 nm have been observed for both samples. The high-resolution TEM imaging confirms the homogenous morphology of the nanoparticles and their crystalline nature. Diffraction fringes were observed throughout the entire sample: the bright spots in the fast Fourier transform image of the nanoparticles, marked in the Fig. 1c, d of the same figure, are easily indexed to the alternation of 3.5 Å spaced (101) planes of the anatase lattice.

The success of the grafting procedure was tested by Raman spectroscopy: results for the bare and grafted titania nanoparticles are shown in Fig. 2.

Raman spectra highlight the occurrence of the typical vibrational features of the anatase lattice ( $396$ ,  $516$ , and  $639\ cm^{-1}$ ) [31] and, for the  $TiO_2-RSO_3H$  grafted filler, also a single peak at  $1046\ cm^{-1}$  likely due to the symmetric stretching mode of  $SO_3^{3-}$  ion [32] and two peaks at about  $2890$  and  $2936\ cm^{-1}$  due to vibrational modes of the aliphatic chain [33].

Prior to proceed to advanced characterization by NMR and other techniques, the morphologies of the pure sPEEK and the composite membranes were characterized by AFM at room temperature and 33 % RH. Examples of phase images of the

**Fig. 1** TEM images at low magnification of  $\text{TiO}_2$  (a) and  $\text{TiO}_2\text{-RSO}_3\text{H}$  (b), and at high magnification together with fast Fourier transform (FFT) image of  $\text{TiO}_2$  (c) and  $\text{TiO}_2\text{-RSO}_3\text{H}$  (d)



pure sPEEK and composite membranes are shown in Fig. 3 together with the statistical image analysis of the sizes of the dark and bright areas.

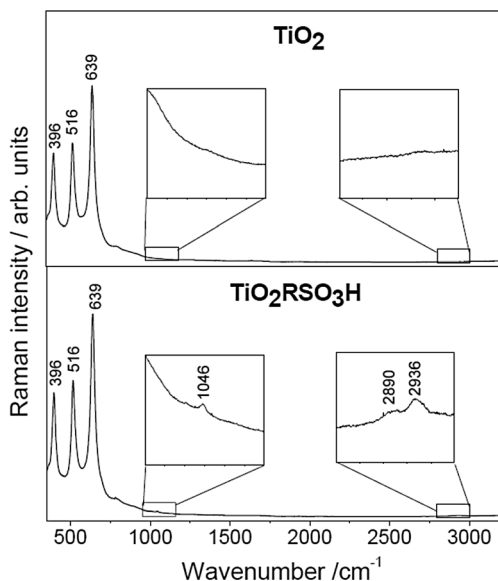


**Fig. 2** Raman spectra of the bare (top panel) and grafted (bottom panel) titania nanopowders. Note the occurrence of vibrational modes of both  $\text{SO}_3^{3-}$  ion and aliphatic chain in grafted powders

As expected, the AFM phase images of the skin layer of the pure and composite sPEEK membranes show a regular alternation of elongated pseudocircular bright and dark areas. This alternation is related to the different hardness/elastic properties of the hydrophobic and hydrophilic domains [34, 35]. Dark areas are assigned to softer regions, which represent the hydrophilic sulphonic group clusters whereas bright areas are attributed to the hard character of (a) the hydrophobic polymer matrix or (b) the filler nanoparticles [36]. The homogeneous dispersion of the dark/bright areas suggests a uniform dispersion of the filler nanoparticles and the lack of filler agglomeration on the membrane surface [36–38].

Analysis of the distributions of the bright and dark domain sizes suggests for both the hydrophobic and hydrophilic cases a lognormal distribution peaked between 11–13, 9–11, and 5–7 nm for the sPEEK, sPEEK/ $\text{TiO}_2$ , and sPEEK/ $\text{TiO}_2\text{-RSO}_3\text{H}$  samples, respectively, with a smooth decreasing tail due to few large pseudo-particles. Hydrophilic domains are in all cases slightly larger than the hard hydrophobic regions. The size of the hydrophilic domains as well as the hydrophobic ones shows a monotonic decreasing trend passing from pure sPEEK to the  $\text{TiO}_2$  and the  $\text{TiO}_2\text{-RSO}_3\text{H}$  composite membranes. Apparently, the incorporation of both inorganic fillers leads to a contraction of the cluster size on the membrane surfaces. This observation suggests that the interaction

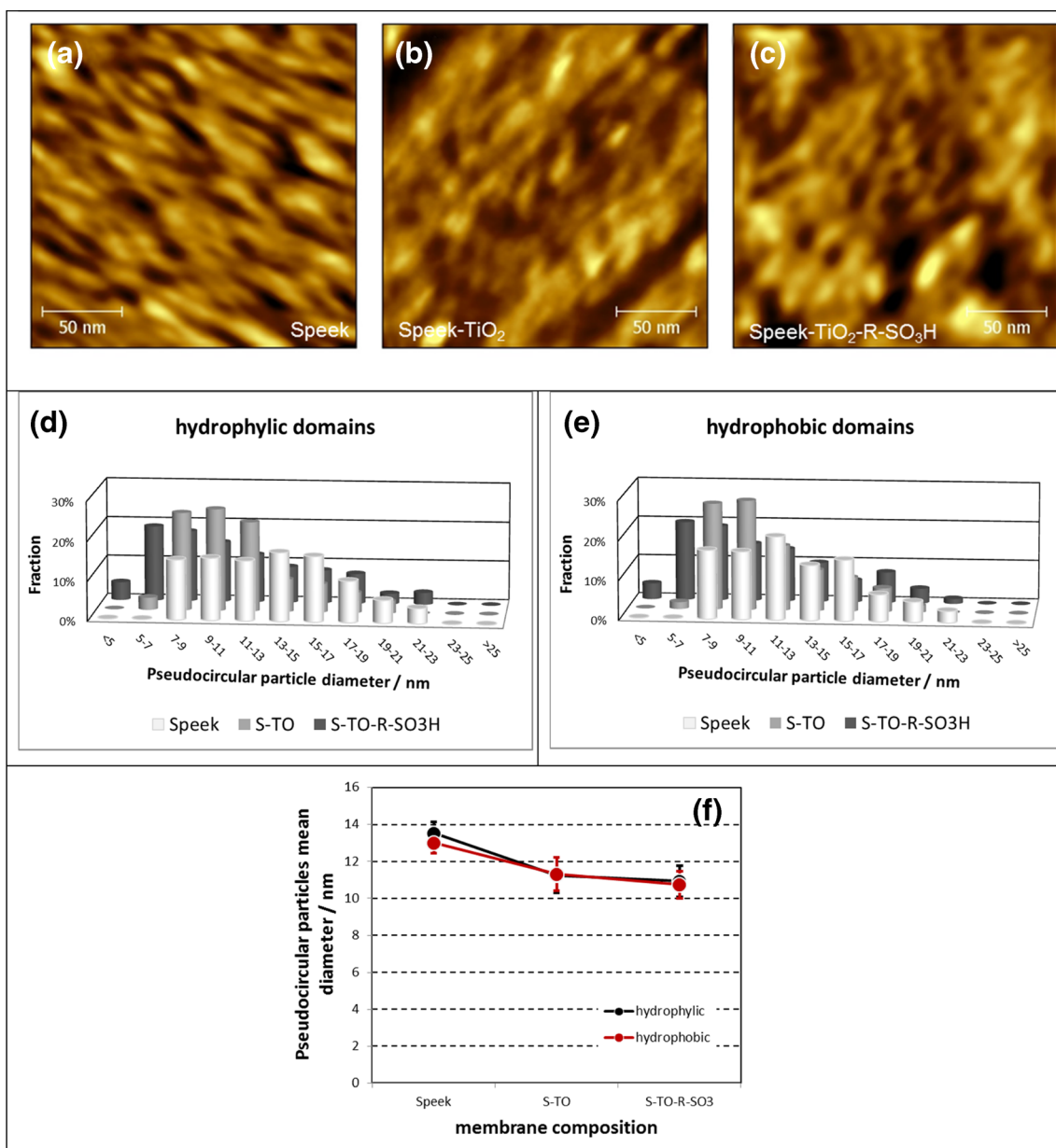


**Fig. 3** a–c AFM-phase images at RH 33 % of pure sPEEK and composite membranes; d hydrophilic and e hydrophobic domain diameter distributions and f mean sizes

between the filler surfaces and the sulphonic acid groups of the polymer decreases the free volume of the hydrophilic regions which are able to contain water as similarly observed by Zhang et al. [39]. On the other hand, it is likely that the reduced size of the hydrophobic/hydrophilic domains may lead to a more interconnected microstructure of the ion conducting channels, thus possibly improving the homogeneity of the surface hydration [40].

**Dynamic mechanical analysis**

The viscoelastic behavior of the membranes was quantified in terms of storage modulus, loss modulus, and loss factor ( $\tan \delta$ ).

The measurements have been collected in the temperature range between 25 and 250 °C, both in heating and in cooling scans. Figure 4a reports the temperature evolution of storage modulus of the sPEEK membrane and of the nanocomposites, sPEEK/TiO<sub>2</sub> and sPEEK/TiO<sub>2</sub>-RSO<sub>3</sub>H. The pure sPEEK shows  $E'$  modulus of  $1.4 \times 10^9$  Pa at room temperature and, during heating, it gradually decreases. sPEEK/TiO<sub>2</sub> has a comparable initial  $E'$  value, but it slightly increases upon heating up to about 80 °C, before declining. sPEEK/TiO<sub>2</sub>-RSO<sub>3</sub>H displays a larger storage modulus value (about  $1.8 \times 10^9$  Pa) and a plateau up to ca. 175 °C. These results demonstrate that the titania filler in the polymer matrix improves the mechanical properties of the membrane, and in particular, the particle’s

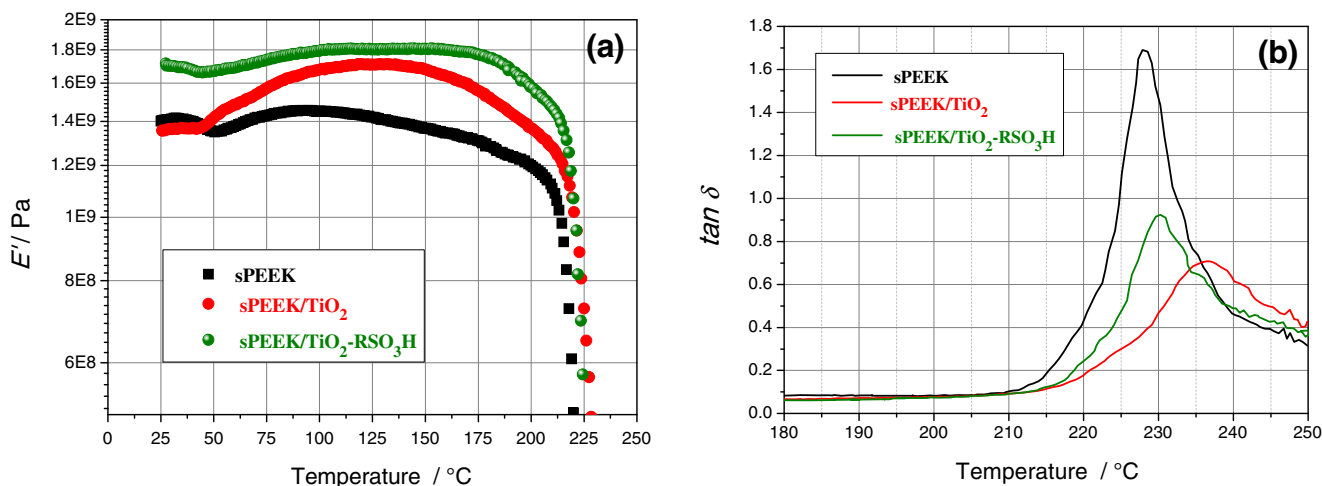


**Fig. 4** Storage modulus  $E'$  (a) and  $\tan \delta$  (b) versus temperature of pristine sPEEK and sPEEK/TiO<sub>2</sub> and sPEEK/TiO<sub>2</sub>-RSO<sub>3</sub>H nanocomposite membranes

functionalization with silylpropylsulfonic groups further enhances the stiffness of the final composite. This beneficial effect is likely due to stronger intermolecular interactions between the polymeric chains. Upon cooling, the storage modulus in all the three samples recovers the same initial values, thus suggesting a complete thermo-reversibility of the mechanical properties for these systems. Turning to the  $\tan \delta$  profile (Fig. 4b), a simple alpha transition is observed for all samples in this temperature range, likely correlated to segmental motions of polymer backbone chains. Whereas for pristine sPEEK membrane, the glass transition temperature is at 228  $^{\circ}\text{C}$ , the nanocomposites both show a slight shift of the  $T_g$  to higher temperatures, in particular the sPEEK/TiO<sub>2</sub>, and also a strong decrease in the loss tangent values from 1.6 to 0.7–0.8. This reduction is likely related to the higher stiffness of the nanocomposites respect to the filler-free membrane.

### NMR investigation

NMR technique has been applied in this study to investigate the transport properties of water and methanol confined in the membranes, with particular emphasis on the effect of the nanoadditives. Figure 5 displays the plots of the water self-diffusion coefficients ( $D$ ) and the relaxation times ( $T_1$ ) measured on completely swelled membranes, in the temperature range 20–130  $^{\circ}\text{C}$ .

At the maximum swelling, the percentage of water uptake is estimated to be 50 % for sPEEK, 42 % for the sPEEK/TiO<sub>2</sub>, and 37 % for the sPEEK/TiO<sub>2</sub>-RSO<sub>3</sub>H, respectively, as reported in the graph's legend. Apparently, the nanocomposite membranes adsorb significant less amount of water compared to the recast sPEEK membrane. This swelling's reduction may well be related to the higher rigidity of the hybrid membranes, because the incorporation of fillers in the polymeric matrix, and especially the presence of sulfonic groups, allows a

greater cross-linking between the polymer chains, with the result of a stiffer membrane, less able to swell.

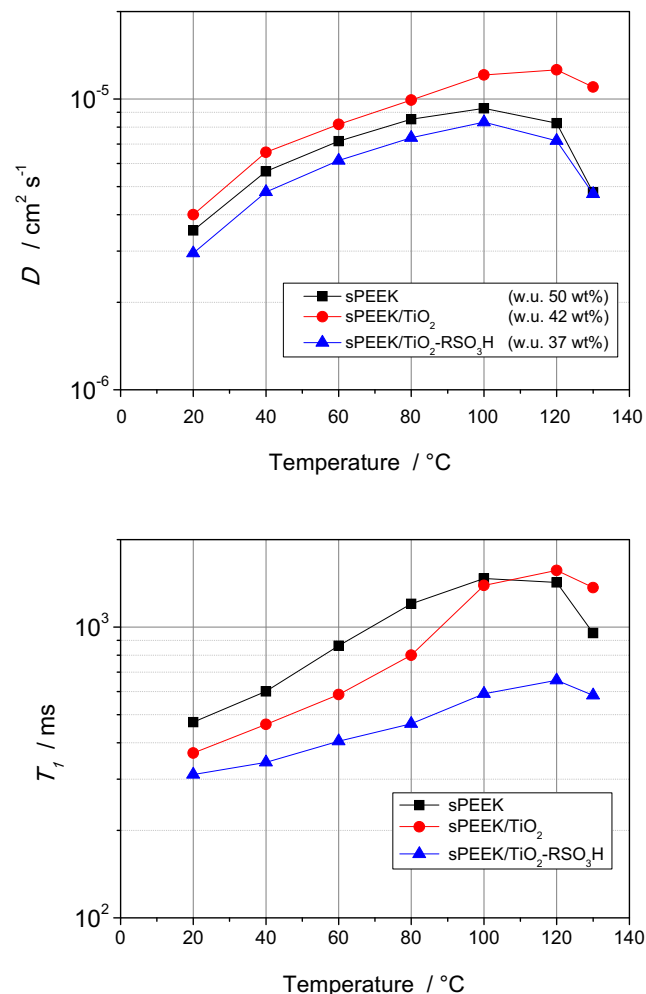


**Fig. 5** Self-diffusion coefficients (top) and longitudinal relaxation times (bottom) of water measured in completely swelled membranes, in the temperature range 20–130  $^{\circ}\text{C}$

The strong relationship between water uptake of the polymer electrolyte and self-diffusion coefficients is well known [41–43]: generally, at room temperature, electrolyte membranes that absorb more water exhibit higher diffusivity. However, in this case, we observe higher water diffusion in the sPEEK/TiO<sub>2</sub> composite, even though the water uptake is smaller than the filler-free sPEEK. Additionally, it increases up to 120 °C and then, due to the water evaporation, decreases rapidly.

At a first glance, it seems peculiar that the presence of sulphonic acid groups on the particles does not enhance the water mobility of the membrane. A possible explanation is that the polymeric chains strongly interact with the TiO<sub>2</sub>-RSO<sub>3</sub>H particles through the sulfonic groups with the result to reduce the filler's hydrophilic active area. This explanation matches well with the apparent reduction of the hydrophilic domain size due to incorporation of the filler and the possible reduction of the free volume able to contain water.

In fact, the sulfonic acid groups, bounded on an aliphatic chain before grafted in titania, may lead to a much better filler dispersion in the recast procedure due to the higher affinity with the organic solvent and polymeric chain.

Further information about the molecular dynamics is provided by measurements of longitudinal (or spin–lattice) relaxation times ( $T_1$ ).  $T_1$  is more sensitive to localized motions in comparison with standard diffusion, including both translation and rotation on a time scale comparable to the reciprocal of the NMR angular frequency ( $\sim 1$  ns). As the molecular correlation time  $\tau_c$  depends on temperature, a minimum in  $T_1$  is often observed when  $\omega\tau_c \sim 1$ , where  $\omega$  is the NMR frequency [44]. In the temperature range investigated, well above the  $T_1$  minimum, i.e., in the so-called extreme narrowing limit ( $\omega\tau_c \ll 1$ ), higher  $T_1$  values suggest more facile molecular motions.

In both the composites,  $T_1$  values are shorter than the pristine sPEEK in almost all the temperature range investigated. This provides an evidence for stronger interactions between the water molecules and the nanoadditives, in particular when they are sulfonated, decreasing their molecular motions. This can be hypothesized in the case of sPEEK/TiO<sub>2</sub>-RSO<sub>3</sub>H

composite to explain the low  $T_1$ , and it is in agreement with the conductivity data reported in the next section.

Turning to the methanol dynamics throughout the membranes, apparently the use of titania nano-filler, leads to major alterations. Figure 6 displays the diffusion coefficients of water and methanol measured in the swollen membranes of sPEEK (Fig. 6a), sPEEK/TiO<sub>2</sub> (Fig. 6b), and sPEEK/TiO<sub>2</sub>-RSO<sub>3</sub>H (Fig. 6c), respectively, in the range of 20–130 °C.

For this study, the membranes were equilibrated in aqueous methanol solution at concentration of 2 M, so as to have the same conditions used in the DMFC cell. Furthermore, in order to discriminate in the <sup>1</sup>H NMR spectrum between the proton signals coming from water or methanol, we used deuterated molecules, i.e., mixture of CH<sub>3</sub>OD/D<sub>2</sub>O and CD<sub>3</sub>OD/H<sub>2</sub>O for measuring methanol and water, respectively [6, 45].

Diffusion coefficients of water and methanol in the sPEEK membrane (Fig. 6a) are overlapped up to 60 °C, and above this temperature, the methanol mobility becomes much higher than that of the water. This behavior is consistent with the methanol crossover observed in the direct methanol fuel cell operation. The sPEEK/TiO<sub>2</sub> (Fig. 6b) shows a different behavior where the water diffusion dominates up to 100 °C, proving the beneficial methanol blocking effect of the nanoparticles dispersed in the polymer. However, above 100 °C, likely due to the solvents evaporation, we observe a brusque decline of the water mobility while the methanol molecules maintain a very high diffusion. On the other hand, the sPEEK/TiO<sub>2</sub>-RSO<sub>3</sub>H membrane shows drastically improved performances: water diffusion is always larger than methanol in the whole investigated temperature range.

We can speculate that the sulfonic groups on the titania particles interacting with the polymer chains cause a higher reticulation, reducing the dimension of the pores and significantly increasing the tortuosity of the diffusional paths of methanol molecules. Obviously, obstruction of the diffusion channels may also affect the diffusive path of bulk water. However, protons can be transported additionally through a Grotthus-type mechanism that is likely enhanced

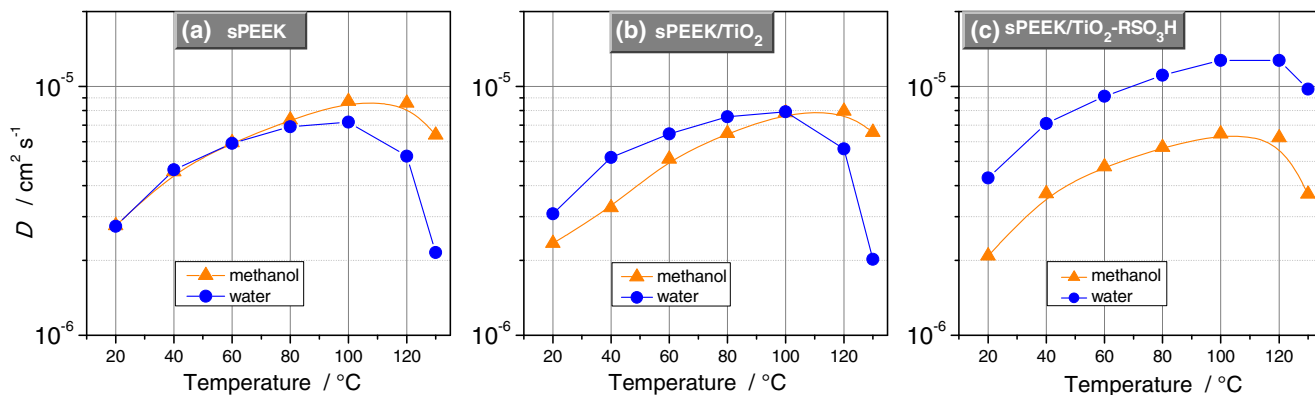


**Fig. 6** Self-diffusion coefficients of water and methanol in 2 M solution confined in sPEEK (a), sPEEK/TiO<sub>2</sub> (b), and sPEEK/TiO<sub>2</sub>-RSO<sub>3</sub>H (c) membranes, respectively, from 20 up to 130 °C

in highly reticulated system: as a final result, the water diffusion coefficients remain higher than methanol also at high temperatures. Additionally, we should be considered that methanol molecules have higher sterical hindrance than that of water molecules.

The concept of tortuosity and porosity of the membranes may be easily made quantitative by considering the ratio of the water self-diffusion coefficients in the ionomers ( $D$ ) and the self-diffusion coefficient of pure water ( $D^0$ ) according to the scaling equation (Eq. 5) [46–48]:

$$D = \frac{\varepsilon}{\tau} D^0 \quad (5)$$

Tortuosity  $\tau$  and porosity  $\varepsilon$  are phenomenological scaling parameters. The porosity is by definition below 1; the tortuosity is defined above 1, where the value 1 would correspond to perfectly straight diffusion paths inside the membrane. The estimation of  $\varepsilon/\tau$  ratios for the three membranes, sPEEK, sPEEK/TiO<sub>2</sub>, and sPEEK/TiO<sub>2</sub>-RSO<sub>3</sub>H, was executed by considering the diffusion coefficients measured at 20 °C, obtaining the following values: sPEEK 0.17, sPEEK/TiO<sub>2</sub> 0.20, and sPEEK/TiO<sub>2</sub>-RSO<sub>3</sub>H 0.14.

Such values confirm our description of such systems: the larger ratio for sPEEK/TiO<sub>2</sub> might correspond to a higher porosity, due to the Titania clusters dispersed, while the sulfonic groups on the particles, through strong reticulations with the polymer, shrink the dimension of the pores, so the porosity is reduced and, likely, tortuosity increases.

Figure 7 shows the plot of the longitudinal relaxation times ( $T_1$ ) vs. temperature of the methanol. These data confirm what affirmed above, i.e., in sPEEK/TiO<sub>2</sub>-RSO<sub>3</sub>H methanol shows the shorter  $T_1$ , implying that its local mobility is reduced, which in turn can be attributed to structuring and nanomorphology of the composite.

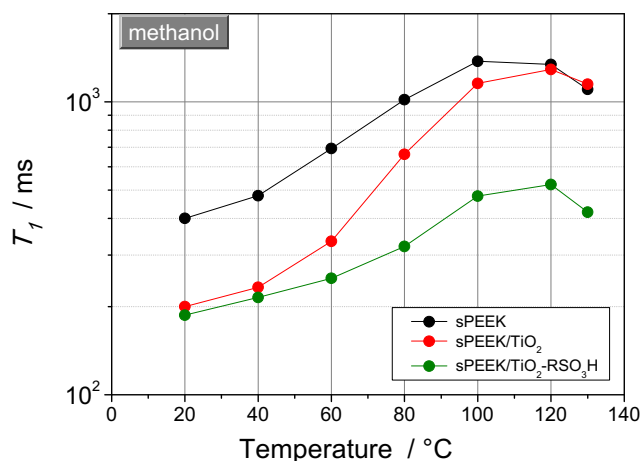


**Fig. 7** Longitudinal relaxation times ( $T_1$ ) of methanol measured in the three membranes swollen in 2 M solution in the temperature range from 20 to 130 °C

Finally, Fig. 8 reports the high-pressure NMR diffusion measurements performed on the membranes equilibrated in aqueous methanol solutions. The three plots compare methanol and water self-diffusion coefficients obtained as a function of the pressure from 1 atm. up to 2 kbar. The measurements were conducted at two different temperatures, 303 and 328 K, but here, only data at 328 K are shown. The aqueous methanol solution uptakes of the membranes were estimated to be about 55 % for sPEEK, 44 % for the sPEEK/TiO<sub>2</sub>, and 38 % for the sPEEK/TiO<sub>2</sub>-RSO<sub>3</sub>H, respectively. Also, in this case, a picture similar to the previous cases is observed: dispersion of nanoparticles in the polymer matrix produces a structure that inhibits the methanol transport; moreover, the functionalization of these particles with the RSO<sub>3</sub>H groups, further enhances the obstruction effect.

Table 1 reports the activation volumes of water and methanol in 2 M solution, respectively, calculated from the diffusion data for the pure sPEEK and the two composites according to Eq. 6:

$$\Delta v = -kT \left( \frac{\partial \ln D}{\partial P} \right)_T \quad (6)$$

Higher activation volume implies that more cooperative motion and hence larger change in local volume is required for the process of diffusion to occur within the membrane. This is consistent with interactions occurring between the methanol molecules and the surface of the nanoparticles. In fact, the activation volume of methanol increases in the composites, and the higher value is obtained for the sulfonated one. On the other hand, as expected, while the activation volume of water decreases in the composites, that of methanol increases.

## Electrochemical investigation

The ion exchange capacity values of the membranes were measured to check the effect of the embedding of nanoadditives. As shown in the Table 2, the IEC of the composites was lower than that of pure sPEEK. In particular, the sPEEK/TiO<sub>2</sub>-RSO<sub>3</sub>H membrane showed the lowest value, in agreement with the similar trend observed for the percentage of water uptake discussed previously for the NMR data (50 % for sPEEK, 42 % for the sPEEK/TiO<sub>2</sub>, and 37 % for the sPEEK/TiO<sub>2</sub>-RSO<sub>3</sub>H). This finding can be explained on the basis of filler/polymer interactions. The segregation of protogenic groups, due to H-bonding between the SO<sub>3</sub>H groups of sPEEK and Si–OH and SO<sub>3</sub>H groups of TiO<sub>2</sub>-RSO<sub>3</sub>H, reduces the amount of the ion exchange functionalities that are responsible for water and methanol uptakes.

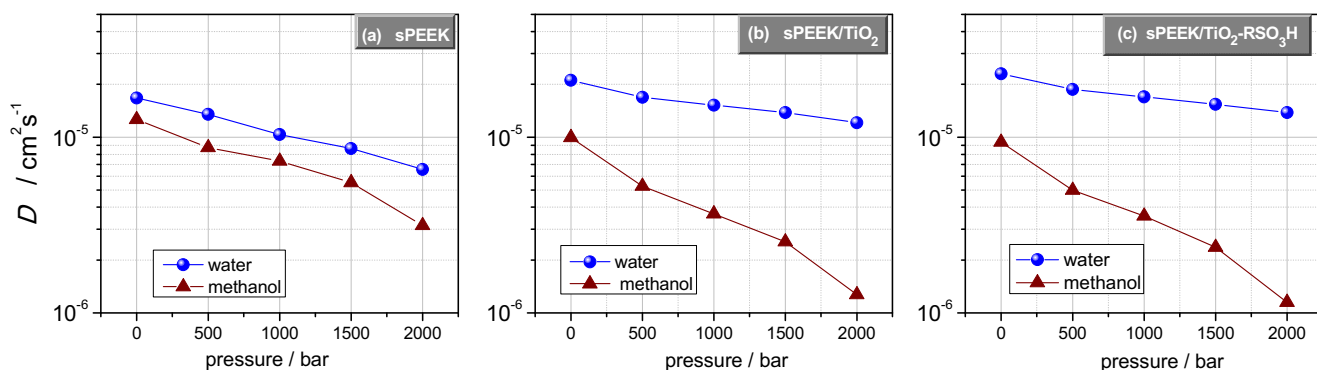


**Fig. 8** Self-diffusion coefficients of water and methanol in 2 M solution confined in sPEEK (a), sPEEK/TiO<sub>2</sub> (b), and sPEEK/TiO<sub>2</sub>-RSO<sub>3</sub>H (c) membranes, respectively, measured by high pressure SE-NMR technique from 0 up to 2 kbar, at 55 °C

The number of water molecules per sulphonic acid group was estimated by the following Eq. 7 and is reported in Table 2:

$$\lambda = \frac{n_{\text{H}_2\text{O}}}{n_{\text{SO}_3\text{H}}} = \frac{10 \times \text{WU}\%}{18 \times \text{IEC}} \quad (7)$$

The decrement of  $\lambda$  value is consistent with narrowing of the ionic clusters for the composite membranes, as observed by AFM analysis.

The proton conductivity of the membranes was measured by EIS and the resulting plots are shown in Fig. 9. As pointed out by the comparison of data relative to the sPEEK/TiO<sub>2</sub> and sPEEK/TiO<sub>2</sub>-RSO<sub>3</sub>H membranes, the functionalization of TiO<sub>2</sub> avoids the reduction of the overall proton conductivity of the electrolyte due to the use of nonconductive inorganic filler.

In the whole investigated temperature range, the sPEEK/TiO<sub>2</sub>-RSO<sub>3</sub>H membrane showed a conductivity similar to that of pure sPEEK, up to 0.04 S cm<sup>-1</sup> at 100 °C, despite its lower values of IEC and water self-diffusion coefficient. This behavior can be explained considering that in the sPEEK/TiO<sub>2</sub>-RSO<sub>3</sub>H membrane, the presence of silylpropylsulfonic groups onto TiO<sub>2</sub> surface leads to a highly reticulated microstructure creating tortuosity and narrowing of the diffusional paths of water molecules. It is thus expected that the contribution to

proton conductivity due to vehicular mechanism, that is the diffusion of protonated water molecules, will be smaller and the relative contribution of the Grotthus-type mechanism will be larger.

DMFC single-cell measurements were carried out to test the functioning of these membranes in a real device. To check the methanol permeability, steady-state limiting methanol oxidation current density ( $J_{\text{lim}}$ ) through the membranes was measured. Figure 10 displays the voltammetric curves resulting from electro-oxidation of methanol permeating through the membranes; the  $J_{\text{lim}}$  value corresponds to the current density plateau.

Methanol permeability decreased in both the composite membranes and, in particular, sPEEK/TiO<sub>2</sub>-RSO<sub>3</sub>H showed the lowest permeability, in agreement with its lowest value of methanol self-diffusion coefficient. The physical cross-linking between the functionalized titania nanoparticles and the polymer chains reduce the size of the hydrophilic channels and thus effectively decreases the methanol permeability that strongly depends on the size and tortuosity of diffusional channels network [49].

Finally, Fig. 11 shows polarization curves ( $I$ - $V$ ) and power density ( $PD$ ) of the membranes, at 70 °C and 1 abs bar.

The sPEEK/TiO<sub>2</sub>-RSO<sub>3</sub>H composite showed better performance than those of the other membranes, in terms of higher power density delivered and reduced methanol crossover. These results are in agreement with the diffusion data previously observed. In this membrane, a larger tortuosity of the diffusive path produces a lower methanol crossover and lower potential losses at low current density. Furthermore, the higher

**Table 1** Activation volumes of water (2 M) and methanol (2 M) in the three membranes and at two temperatures

Membrane	Activation volume (cm <sup>3</sup> mol <sup>-1</sup> )			
	H <sub>2</sub> O/CD <sub>3</sub> OD (2 M)		D <sub>2</sub> O/CH <sub>3</sub> OD (2 M)	
	303 K	328 K	303 K	328 K
sPEEK	16.5	12.0	21.5	16.7
sPEEK/TiO <sub>2</sub>	11.6	6.8	28.6	25.1
sPEEK/TiO <sub>2</sub> -RSO <sub>3</sub> H	10.4	6.3	30.2	25.6

The error bar for these volumes is around ±0.5 (since the error on  $D$  values of about 3 %)

**Table 2** Ion exchange capacity (IEC) values and hydration number ( $\lambda$ ) of the membranes

Membrane	IEC (meq/g)	$\lambda$
sPEEK	1.73	16
sPEEK/TiO <sub>2</sub>	1.53	15
sPEEK/TiO <sub>2</sub> -RSO <sub>3</sub> H	1.44	14

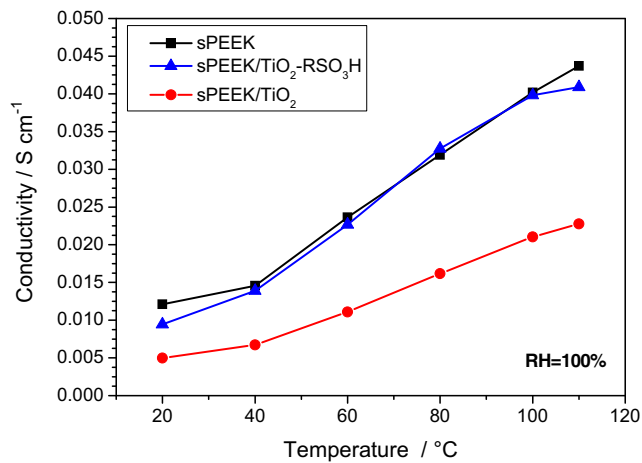


**Fig. 9** Proton conductivity of pure sPEEK and composite membranes

water mobility with respect to that of methanol and the significant contribution of the Grotthuss-type mechanism to the proton conductivity ensure a lower resistance and thus the possibility to produce higher current density in a DMFC.

The polarization and power density curves of the membranes, recorded at 90 °C and 2 abs bar, are shown in Fig. 12.

As can be observed, the maximum *PD* of the cell increase with increment of the temperature and pressure for all the sPEEK-based membranes. In detail, the sPEEK/TiO<sub>2</sub>-RSO<sub>3</sub>H composite showed the best performance also in these operating conditions ( $PD_{\max} = 40 \text{ mW cm}^{-2}$  and  $I_{(0.2 \text{ V})} = 200 \text{ mA cm}^{-2}$ ), with a *PD* improvement of 20 % with respect to the pure sPEEK membrane. As highlighted by NMR measurements, the sPEEK/TiO<sub>2</sub>-RSO<sub>3</sub>H membrane showed the highest value of the water self-diffusion coefficient and the lowest value of that of methanol, in comparison with the other membranes. This is consistent with the highest current and power density by the cell equipped with the sPEEK/TiO<sub>2</sub>-RSO<sub>3</sub>H composite.

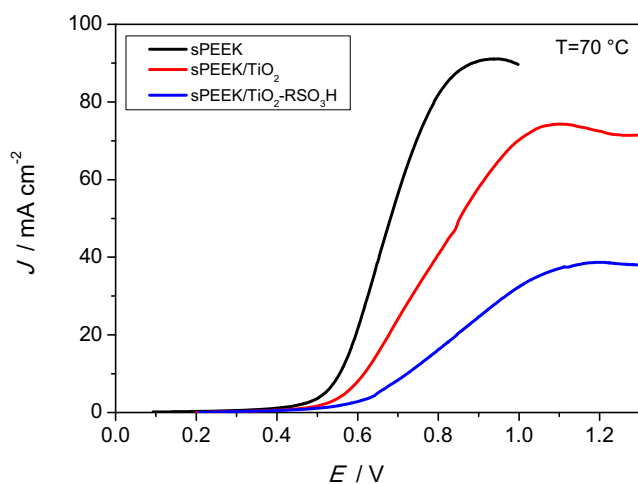


**Fig. 10** Voltammetric curves for the oxidation of methanol permeating through the membranes exposed to a 2 M methanol feed, at 70 °C

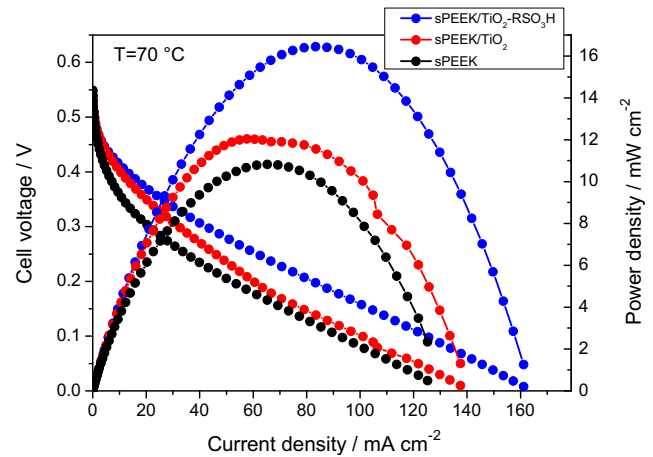


**Fig. 11** DMFC polarization and power density curves at 70 °C for the MEA equipped with composite and pure sPEEK membranes

## Conclusions

Propylsulfonic acid functionalized titania TiO<sub>2</sub>-RSO<sub>3</sub>H was chosen as nanoadditive for the preparation of sPEEK-based composites because the presence of bifunctional branches on the filler surface affects the structuring and nanomorphology of hydrophilic and hydrophobic domains within the membrane, and hence the properties of the electrolyte.

Mechanical analysis performed on the membranes demonstrate that the presence of titania nanoparticles functionalized with silylpropylsulfonic groups enhances the stiffness of the composite, likely due to higher intermolecular interactions among the polymeric chains. This results in a higher reticulation of the polymer matrix, increasing the tortuosity of the diffusional paths for methanol transport, as highlighted from the NMR investigation. On the other hand, the proton acid of water can be transported through the Grotthuss-type mechanism, much more favored in the highly reticulated system.

The functionalization of TiO<sub>2</sub> avoids the detrimental effect on overall proton conductivity of the membranes due to

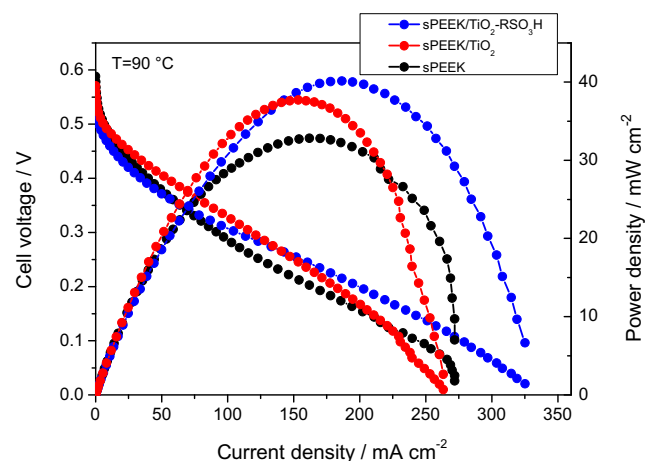


**Fig. 12** DMFC polarization and power density curves at 90 °C for the MEA equipped with composite and pure sPEEK membranes

embedding of the low-conducting ceramic oxide in the polymer matrix. Conductivity measurements showed that the sPEEK/TiO<sub>2</sub>-RSO<sub>3</sub>H membrane exhibits conductivity values similar to those of pure sPEEK and higher than those of sPEEK/TiO<sub>2</sub> membrane in spite of its lower values of water self-diffusion coefficient and ion exchange capacity.

DMFC tests highlighted that the composites show lower methanol permeability than that of pure sPEEK membrane and, at the same filler content, the membranes incorporated with sulfonic acid functionalized titania exhibit much lower methanol permeability as compared with those incorporated with pristine titania nanoparticles.

In conclusion, the higher water mobility with respect to that of methanol within the sPEEK/TiO<sub>2</sub>-RSO<sub>3</sub>H membrane and the considerable contribution to the proton conductivity due to the Grotthuss-type mechanism lead to a good cell response when this electrolyte is used in a DMFC, in terms of reduced methanol crossover and higher current and power density delivered.

This last result is really outstanding if we consider that sPEEK membranes in general show very good methanol resistance and mechanical properties but at the same time suffer from lower proton conductivity compared to Nafion. Finally, using the sulfonated titania filler, we have managed to achieve low methanol permeability without sacrificing the conducting performance of the membrane.

**Acknowledgments** This work was carried out with the financial support of the Italian Ministry of Education, Universities and Research (Project: PRIN 2011, NAMED-PEM). The NMR measurements at Hunter College were supported by a grant from the US Office of Naval Research.

## References

- Wasmus S, Kuver A (1999) Methanol oxidation and direct methanol fuel cells: a selective review. *J Electroanal Chem* 461:14–31
- Aricò AS, Srinivasan S, Antonucci V (2001) DMFCs: from fundamental aspects to technology development. *Fuel Cells* 1:133–161
- Han J, Liu H (2007) Real time measurements of methanol crossover in a DMFC. *J Power Sources* 164:166–173
- Kim JH, Kim SK, Nam K, Kim DW (2012) Composite proton conducting membranes based on nafion and sulfonated SiO<sub>2</sub> nanoparticles. *J Membr Sci* 415–416:696–701
- Kim Y, Choi Y, Kim HK, Lee JS (2010) New sulfonic acid moiety grafted on montmorillonite as filler of organic–inorganic composite membrane for non-humidified proton-exchange membrane fuel cells. *J Power Sources* 195:4653–4659
- Nicotera I, Simari C, Coppola L, Zygouri P, Goumis D, Brutti S, Minuto FD, Aricò AS, Sebastian D, Baglio V (2014) Sulfonated graphene oxide platelets in Nafion nanocomposite membrane: advantages for application in direct methanol fuel cells. *J Phys Chem C* 118:24357–24368
- Nicotera I, Kosma V, Simari C, D’Urso C, Aricò AS, Baglio V (2014) Methanol and proton transport in layered double hydroxide and smectite clay-based composites: influence on the electrochemical behavior of direct methanol fuel cells at intermediate temperatures. *J Solid State Electrochem*. doi:10.1007/s10008-014-2701-y
- Cozzi D, de Bonis C, D’Epifanio A, Mecheri B, Tavares AC, Licocchia S (2014) Organically functionalized titanium oxide/nafion composite proton exchange membranes for fuel cells applications. *J Power Sources* 248:1127–1132
- de Bonis C, Cozzi D, Mecheri B, D’Epifanio A, Rainer A, De Porcellinis D, Licocchia S (2014) Effect of filler surface functionalization on the performance of Nafion/titanium oxide composite membranes. *Electrochim Acta* 147:418–425
- Awang N, Ismail AF, Jaafar J, Matsuura T, Junoh H, Othman MHD, Rahman MA (2015) Functionalization of polymeric materials as a high performance membrane for direct methanol fuel cell: A review. *React Funct Polym* 86:248–258
- Mishra AK, Bose S, Kuila T, Kim NH, Lee JH (2012) Silicate-based polymer-nanocomposite membranes for polymer electrolyte membrane fuel cells. *Prog Polym Sci* 37:842–869
- Villa DC, Angioni S, Quartarone E, Righetti PP, Mustarelli P (2013) New sulfonated PBIs for PEMFC application. *Fuel Cells* 13:98–103
- Roy A, Hickner MA, Einsla BR, Harrison WL, McGrath JE (2009) Synthesis and characterization of partially disulfonated hydroquinone-based poly(arylene ether sulfone)s random copolymers for application as proton exchange membranes. *J Polym Sci Part A: Polym Chem* 47:384–391
- de Bonis C, D’Epifanio A, Di Vona ML, D’Ottavi C, Mecheri B, Traversa E, Trombetta M, Licocchia S (2009) Proton conducting hybrid membranes based on aromatic polymers blends for direct methanol fuel cell applications. *Fuel Cells* 9:387–393
- Laberty-Robert C, Valle K, Pereira F, Sanchez C (2011) Design and properties of functional hybrid organic–inorganic membranes for fuel cells. *Chem Soc Rev* 40:961–1005
- de Bonis C, D’Epifanio A, Di Vona ML, Mecheri B, Traversa E, Trombetta M, Licocchia S (2010) Proton-conducting electrolytes based on silylated and sulfonated polyetheretherketone: synthesis and characterization. *J Polym Sci Part A: Polym Chem* 48:178–2186
- Mollà S, Compañ V (2014) Polymer blends of sPEEK for DMFC application at intermediate temperatures. *Int J Hydrog Energy* 39:5121–5136
- de Bonis C, D’Epifanio A, Mecheri B, Traversa E, Miyayama M, Tavares AC, Licocchia S (2012) Layered tetratitanate intercalating sulfanilic acid for organic/inorganic proton conductors. *Solid State Ionics* 227:73–79
- Jones DJ, Rozière J (2008) Advances in the development of inorganic–organic membranes for fuel cell applications. *Adv Polym Sci* 215:219–264
- Alvarez A, Guzmán C, Carbone A, Saccà A, Gatto I, Passalacqua E, Nava R, Ornelas R, Ledesma-García J, Arriaga LG (2011) Influence of silica morphology in composite Nafion membranes properties. *Int J Hydrog Energy* 36:14725–14733
- Fontanella JJ, Edmonson CD, Wintersgill MC, Wu Y, Greenbaum SG (1996) High-pressure electrical conductivity and NMR Studies in variable equivalent weight NAFION membranes. *Macromolecules* 29:4944–4951
- Fontanella JJ, Wintersgill MC, Chen RS, Wu Y, Greenbaum SG (1995) Charge transport and water molecular motion in variable molecular weight nafion membranes: high pressure electrical conductivity and NMR. *Electrochim Acta* 40:2321–2326
- Jayakody JRP, Stallworth PE, Mananga ES, Zapata JF, Greenbaum SG (2004) High pressure NMR study of water self-diffusion in NAFION-117 membrane. *J Phys Chem B* 108:4260–4262
- Nicotera I, Khalfan A, Goenaga G, Zhang T, Bocarsly A, Greenbaum S (2008) NMR investigation of water and methanol

- mobility in nanocomposite fuel cell membranes. *Ionics* 14:243–253
25. Licoccia S, Traversa E (2006) Increasing the operation temperature of polymer electrolyte membranes for fuel cells: from nanocomposites to hybrids. *J Power Sources* 159:12–20
  26. He Q, Kusoglu A, Lucas IT, Clark K, Weber AZ, Kostecki R (2011) Correlating humidity-dependent ionically conductive surface area with transport phenomena in proton-exchange membranes. *J Phys Chem B* 115:11650–11657
  27. Abramoff MD, Magalhaes PJ, Ram SJ (2004) Image processing with ImageJ. *J Biophoton Int* 11:36–42
  28. Rasband WS (1997–2014) In: ImageJ, U. S. National Institutes of Health, Bethesda, Maryland, USA, <http://imagej.nih.gov/ij/>, 1997–2014
  29. Tanner JE (1970) Use of the stimulated echo in NMR diffusion studies. *J Chem Phys* 52:2523–2526
  30. Stejskal EO, Tanner JE (1965) Spin diffusion measurements: spin echoes in the presence of a time-dependent field gradient. *J Chem Phys* 42:288–292
  31. Giarola M, Sanson A, Monti F, Mariotto G, Bettinelli M, Speghini A, Salviulo G (2010) Vibrational dynamics of anatase TiO<sub>2</sub>: polarized Raman spectroscopy and ab initio calculations. *Phys Rev B* 81:1743051–1743058
  32. Nakamoto K (1986) Infrared and Raman spectra of inorganic and coordination compounds, J. Wiley & Sons, New York
  33. Silverstein R, Bassler G, Morrill TC (1991) Spectrometric identification of organic compounds, J. Wiley & Sons, Toronto
  34. Kim Y, Hickner MA, Dong L, Pivovar BS, McGrath JE (2004) Sulfonated poly(arylene ether sulfone) copolymer proton exchange membranes: composition and morphology effects on the methanol permeability. *J Membr Sci* 243:317–326
  35. Ling X, Jia C, Liu J, Yan C (2012) Preparation and characterization of sulfonated poly(ether sulfone)/sulfonated poly(ether ether ketone) blend membrane for vanadium redox flow battery. *J Membr Sci* 415–416:306–312
  36. Xiao CY, Sun GM, Yan DY, Zhu PF, Tao P (2002) Synthesis of sulfonated poly(phthalazinone ether sulfone)s by direct polymerization. *Polymer* 43:5335–5339
  37. Li X, Zhao C, Lu H, Wang Z, Na H (2005) Direct synthesis of sulfonated poly(ether ether ketone)s (SPEEKs) proton exchange membranes for fuel cell application. *Polymer* 46:5820–5827
  38. Goalawit R, Chirachanchai S, Shishatkiy S, Nunes SP (2008) Sulfonated montmorillonite/sulfonated poly(ether ether ketone) (SMMT/SPEEK) nanocomposite membrane for direct methanol fuel cells (DMFCs). *J Membr Sci* 323:337–346
  39. Zhang Y, Shao K, Zhao C, Zhan G, Li H, Fu T, Na H (2009) Novel sulfonated poly(ether ether ketone) with pendant benzimidazole groups as a proton exchange membrane for direct methanol fuel cells. *J Power Sources* 194:175–181
  40. Brutti S, Scipioni R, Navarra MA, Panero S, Allodi V, Giarola M, Mariotto G (2014) SnO<sub>2</sub>-nafion® nanocomposite polymer electrolytes for fuel cell applications. *Int J Nanotechnol* 11:882–896
  41. Nicotera I, Zhang T, Bocarsly A, Greenbaum S (2007) NMR characterization of composite polymer membranes for low-humidity PEM fuel cells. *J Electrochem Soc* 154:B466–B473
  42. Nicotera I, Enotiadis A, Angjeli K, Coppola L, Ranieri GA, Gournis D (2011) Effective improvement of water-retention in nanocomposite membranes using novel organo-modified clays as fillers for high temperature PEMFCs. *J Phys Chem B* 115:9087–9097
  43. Enotiadis A, Angjeli K, Baldino N, Nicotera I, Gournis D (2012) Graphene-based nafion nanocomposite membranes: enhanced proton transport and water retention by novel organo-functionalized graphene oxide nanosheets. *Small* 8:3338–3349
  44. Slichter C (1990) Principles of magnetic resonance, springer series in solid state science, 3rd edn. York, New
  45. Nicotera I, Angjeli K, Coppola L, Aricò AS, Baglio V (2012) NMR and electrochemical investigation of the transport properties of methanol and water in Nafion and clay-nanocomposites membranes for DMFCs. *Membranes* 2:325–345
  46. Epstein N (1989) On tortuosity and the tortuosity factor in flow and diffusion through porous media. *Chem Eng Sci* 44:777–779
  47. Pasquini AL, Ziarelli F, Viel S, Di Vona ML, Knauth P (2015) Fluoride ion-conducting polymers: ionic conductivity and fluoride ion diffusion coefficient in quaternized polysulfones. *ChemPhysChem*. doi:10.1002/cphc.201500643
  48. Quartarone E, Mustarelli P, Magistris A (2002) Transport properties of porous PVDF membranes. *J Phys Chem B* 106:10828–10833
  49. Pandey RP, Shahi VK (2013) Aliphatic-aromatic sulphonated polyimide and acid functionalized polysilsesquioxane composite membranes for fuel cell applications. *J Mater Chem A* 1:14375–14383